Mechanisms Underpinning Heterogeneous Deconstruction of Circular Polymers: Insight from Magnetic Resonance Methodologies

Shira Haber,[1*] Julia Im,[2] Mutian Hua,[1] Alexander R. Epstein,[3†] Sophia N. Fricke,[2] Raynald Giovine,[4] Hasan Celik,[4] Kristin A. Persson,[1,2,5] Brett A. Helms,[1,5] and Jeffrey A. Reimer[1,2*]

1 Materials Sciences Division, Lawrence Berkeley National Laboratory, Berkeley, CA 94720 USA.

2 Department of Chemical and Biomolecular Engineering, University of California, Berkeley, Berkeley, CA 94720 USA.

3 Department of Materials Sciences and Engineering, University of California, Berkeley, Berkeley, CA 94720 USA.

4 Pines Magnetic Resonance Center, Core NMR Facility, College of Chemistry, University of California, Berkeley, CA, 94720 USA.

5 The Molecular Foundry, Lawrence Berkeley National Laboratory, Berkeley, CA 94720 USA.

ABSTRACT: Circular plastics thrive on the ability to chemically recycle polymers into reusable monomers, ideally closing the loop from manufacturing to end of life. Mechanisms for heterogeneous polymer deconstruction are complex, involving diffusion and transport of reagents to reactive sites in a material continuously undergoing chemical transformations. A deeper understanding of deconstruction phenomena would better inform the molecular basis of circularity in plastics. Here, we show how nuclear magnetic resonance (NMR) spectroscopy, relaxometry, and diffusometry enable monitoring of heterogeneous deconstruction of a model elastomer with acid-cleavable diketoenamine bonds. In chaotropic aqueous HBr, polydiketoenamine (PDK) deconstruction is fast, enabled by macro- and micro-scale swelling in early stages, which facilitates acid penetration and protonation of reaction sites deep within the polymer sample. We observe a previously unrecognized hydrogen-bond stabilized protonated amine intermediate that is persistent throughout deconstruction, and found a strong correlation of its reactivity with swelling and chain kinetics. In kosmotropic aqueous H_2SO_4, PDK deconstruction is notably slower. Swelling occurred at a more gradual pace, creating a porous polymer matrix, yet polymer chain mobility remained low. Most notably, the kosmotropic character of aqueous H_2SO_4 resulted in a reaction site that was comparably less active in advancing hydrolysis and deconstruction to shorter oligomer chains, instead trapping acid in matrix pores and modifying the activity of the reaction medium under confinement in the process.

INTRODUCTION

Circular polymers have emerged as a potential solution to the world's growing disposable plastic waste problem.[1–5] One class of circular polymers are polydiketoenamine (PDK) resins, produced from triketone and amine monomers that condense spontaneously, producing water as the sole byproduct.[6] Deconstruction of these polymers is enabled by a hydrolysis reaction in acid solution, decomposing the material to its initial reusable triketone and amine monomers. The broad palette of triketone and amine monomers available permits the creation of circular thermoplastics, elastomers, and thermosets with unique architectures, as well as useful tunable properties for a range of applications.[1,7] Furthermore, PDK deconstruction is an acid-catalyzed reaction that occurs on spatially- and temporally-evolving interfaces between two thermodynamic phases, and thus poses fundamental questions about non-linear and non-ideal heterogeneous chemical reaction rates. We consider nuclear magnetic resonance (NMR) in its various forms as a non-invasive characterization strategy to study these fundamental phenomena and thus inform circular design of plastics on the basis of both polymers and processes.

PDK (Figure 1a) is an exemplary system for studying polymer deconstruction. Deconstruction rates are known to be affected by the extent of swelling and ionization of polymer chains in acidic media, diffusion of reactants and products within the polymer milieu, solvation of ions in complex multicomponent solutions, and the activation of chemically labile bonds.[5,8–12] Heteroatom substitutions[7,13] and spacing along amine and triketone segments[14] also permit tunable fast hydrolysis rates. The initial stage of polymer deconstruction is governed by swelling of polymer chains, while at later stages, the reaction becomes diffusion mediated, enhanced by activation through hydrogen bonds.[15] Strict separation and deconvolution of the various chemical and thermodynamic factors affecting the deconstruction process is challenging, e.g., the non-linear reaction kinetics being recently described with fractal-like mathematical model.[16] Nonetheless, a full molecular-level understanding of the deconstruction process is still lacking.

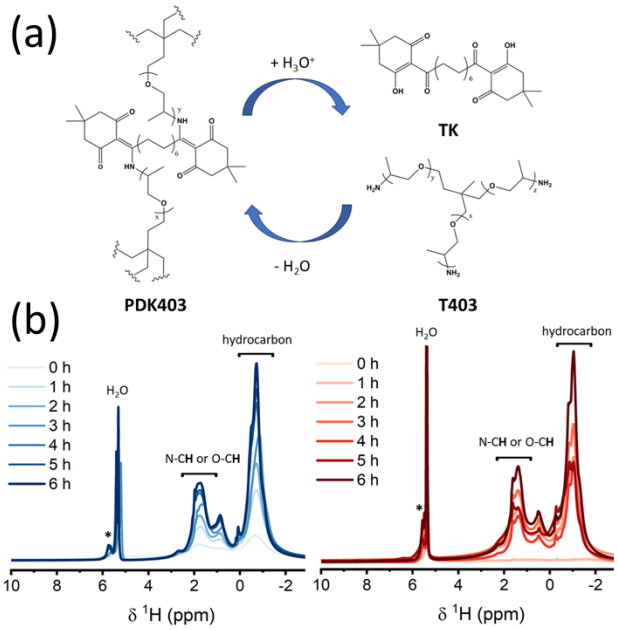

Figure 1. (a) Chemical structure of the deconstruction of polydiketoenamine (PDK403) to its monomers, triamine polypropylene glycol crosslinker (T403) and triketone (TK) and the circular process to create PDK403. (b) In-situ solution-state ^{1}H NMR measurements of PDK403 in 5 M DBr/D_2O (blue) and D_2SO_4/D_2O acid (red) solutions performed at 11.7 T. Chemical environment regions and water peaks are labeled. An asterisk marks the presence of a new environment.

Herein, we monitor molecular transformations of PDK polymers during acid deconstruction with NMR techniques. Two acid solutions were selected: HBr, a chaotropic agent enhancing polymer–water interactions; and H_2SO_4, a kosmotropic agent, increasing surface tension due to low polymer–water interactions.[12,15,17] Consistent with previous bulk studies,[15,16] we find deconstruction rate constants for PDK to follow $k_{HBr} > k_{H2SO4}$. At episodic intervals, we quenched the HBr deconstruction of PDK polymers so as to employ ^{1}H and ^{13}C solid-state NMR (ssNMR) spectroscopy to probe the chemical structure of the recovered deconstructed polymer. A combination of solution- and solid-state multi-nuclei NMR, together with DFT calculations, reveal a reaction intermediate that inhibits further monomer formation, providing a key insight into design of more rapidly degrading PDK constructs. We further use relaxometry and diffusometry NMR methods to assess the molecular mobility of PDK and its fragments as a function of deconstruction time, thereby revealing the mobility of specific chemical environments throughout the activation of the diketoenamine bond. Our results point to a previously unrecognized mechanism for ensuring circularity in plastics undergoing heterogeneous deconstruction: control over local chain mobility is critical in overcoming barriers in accessing reactive conformations. Our results also suggest that there are molecular-informed strategies for co-designing polymers and process to deliver reusable monomers in high yield and purity at fast overall rates by considering macromolecular dynamics and conformation.

RESULTS AND DISCUSSION

We monitored acid deconstruction of a PDK elastomer (PDK403) prepared from a simple ditopic triketone (TK) monomer and a triamine polypropylene glycol crosslinker with an average molar mass of 440 g mol^{-1} (T403) in an acidic medium via three methods. Firstly, we carried out *in-situ* solution state NMR, probing the small molecules being released in solution during the course of the reaction. During the early stages of PDK403 deconstruction in acid, the polymer consists of a hydrophobic solid material with minimal ^{1}H solution-state NMR signal. As deconstruction progresses, the soluble intermediates show an increase in NMR signal intensity, governed by their acid solubility, until the TK final monomer, an insoluble solid, precipitates and the solution-state NMR signal is lost. The rise and fall of these solution-state NMR signals thus follows soluble reaction intermediates. Secondly, we carried out multi-nuclear solid-state NMR measurements on solid polymer samples deconstructed for specific reaction times. The deconstructed polymer, consisting of only the distended outer layer of material that reacted with the acid, was subject to the solid-state NMR experiments. Thirdly, we carried out spin-lattice relaxation measurements in the rotating frame (^{1}H $T_{1\rho}$ relaxation) and *in-situ* pulsed field gradient (PFG) NMR, diagnosing dynamic morphological heterogeneity of the polymer during the deconstruction process.

In-situ characterization

A circular punch (8 mm diameter and 1 mm height) of PDK403 elastomer (Figure 1a), was placed in 5 M deuterated acid solution in an NMR tube and monitored hourly with solution-state ^{1}H NMR (Figure 1b). Note that a shift of ~ 2 ppm upfield of the proton resonances occurs as a result of the presence of high concentrated acids (Figure S1).

At t=0 h (the time of acid addition), a very small ^{1}H signal is detected for the polymer in both acid solutions, as expected for the insoluble hydrophobic PDK403 polymer (^{1}H NMR spectrum of PDK403 in D_2O can be found in Figure S2). Organic solvents lead to swelling of the polymer chains and do not further dissolve the polymer (Figure S3). As deconstruction progresses, growth in proton signals emanating from the hydrocarbon region, –2 to 0.5 ppm (0–2.5 ppm in $CDCl_3$, Figure S1), and the heteroatom region (N-CH and O-CH), 1 to 3 ppm (3–5 ppm in $CDCl_3$, Figure S1), is evident. These increases are the result of polymer protonation and further solvation and a decrease in hydrophobicity. These liquid-state NMR measurements do not show a significant spectral difference between the two acids.

Interestingly, a peak resonating at 5.5 ppm in D_2SO_4 and 5.8 ppm in DBr (Figure 1b, asterisk) emerges and grows with reaction time. The chemical shift suggests that this peak emanates from the protonated amine that detaches from the polymer. Indeed, the protonated state of the crosslinker monomer T403 ($-NH_3^+$) is soluble in both acids

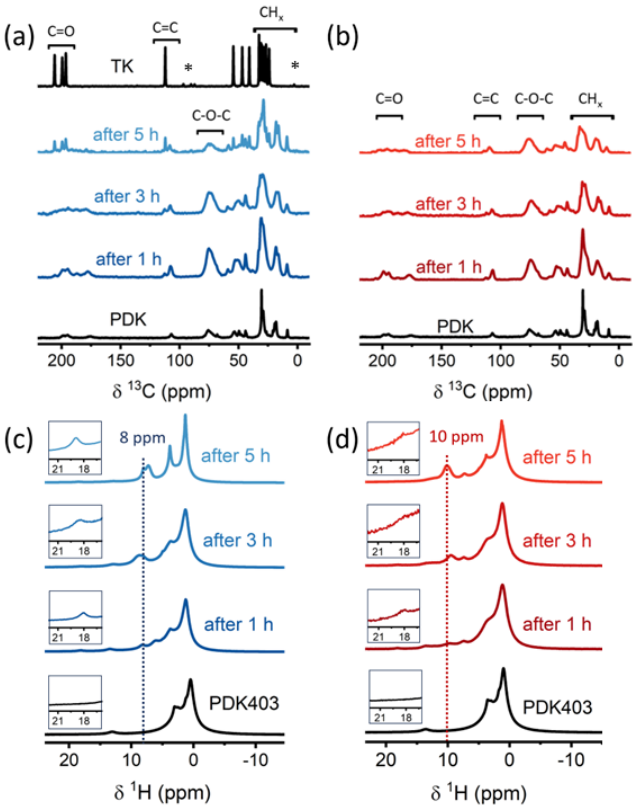

Figure 2. ^{1}H–^{13}C multi-CP spectra of recovered PDK403 after different deconstruction times in (a) 5 M HBr solution (blue) and (b) 5 M H_2SO_4 solution (red) acquired at 9.4 T. Various chemical environments are labelled. Normalization according to number of scans and sample weight was performed. Spinning sidebands are marked with an asterisk. ^{1}H Hahn echo spectra of recovered PDK403 after different deconstruction times in (c) 5 M HBr solution (blue) and (d) 5 M H_2SO_4 solution (red) acquired at 9.4 T. Insets magnify the 18 ppm peak assigned to the monomer enol proton environment. Normalization was performed according to number of scans and sample weight.

(Figure S4). TK monomers, however, are not soluble in acid solutions and precipitate or float to the acid surface. Figure S5 shows the lack of ^{1}H signal from the measurement of TK in deuterated acid/D_2O as compared to ^{1}H spectrum of TK in $CDCl_3$. We conclude that the molecular origin of the new peak is unclear from these solution NMR data alone, and the differing solubilities of the various species (polymers, monomers, and deconstructed intermediates) during the deconstruction process establish the need for further analyses.

Polymer Deconstruction Pathways from Solid-state NMR

In-depth investigation of polymer deconstruction, with high resolution and high sensitivity, was enabled with multi nuclear solid-state NMR measurements performed on deconstructed polymer samples that consist of only the distended outer layer of material that reacted with acid (detailed sample preparation can be found in Materials and Methods section and Figure S6). Figure S7 shows the comparison of in-situ and ex-situ NMR spectra for ^{1}H and ^{13}C measurements, demonstrating that the integrity of the sample remains with both measurement setup conditions. Figure 2a and 2b show the quantitative ^{1}H-^{13}C multi-CP[18–20] measurements of the recovered deconstructed polymer in 5 M HBr and 5 M H_2SO_4, respectively. Four regions of interest have been labelled as follows: methylene CH_x moieties resonating at 0–40 ppm that correspond to carbons of the polymer chains; C-O-C, ether carbons resonating at 65–75 ppm; C=C double bonds resonating at 105–115 ppm; and C=O, carbonyls resonating at 170–210 ppm. Clear changes in carbon environments are evident as a function of polymer deconstruction time in HBr.

Peaks associated with methylene CH_x groups become broader with reaction time, yet after 5 h sharpen and narrow. The ether region's signal intensity decreases with time, likely a result of elimination of the protonated amine crosslinker. After one hour in acid, new peaks emerge that originate from TK monomer formation (shown in first stacked row), growing in intensity as deconstruction advances. As the reaction proceeds past five hours, polymer chain linewidth decreases, particularly for the HBr-reacted system. This is presumed to be associated with increased mobility of the monomer-like CH_x bonds, further supporting the enhanced deconstruction rate of PDK in HBr acid medium, and will be discussed further. In comparison, ^{13}C spectra of deconstructed polymer in H_2SO_4 acid show very subtle changes. A small peak at 112 ppm (C=C bond) emerges after 1 h but does not grow with deconstruction time, indicating that hydrolysis is taking place, but at a much slower rate.

Enhanced deconstruction kinetics in HBr vis-á-vis H_2SO_4 can also be seen from fast magic angle spinning (MAS) quantitative ^{1}H Hahn echo measurements plotted in Figure 2c and 2d. PDK403 shows two broad overlapping peaks in the 0–4 ppm region, corresponding to CH_3, CH_2 and CH_2-O bonds, and the amine proton that resonates at 13.6 ppm. After 1 h deconstruction in both acids, a new peak emerges at 18 ppm, which is assigned to the enol proton of the TK monomer (Figure 1a and S8). Two small new proton peaks are observed in H_2SO_4 deconstruction (red). The first peak, resonating at 7.4 ppm, is assigned to protonated amine, $-NH_3^+$ (Figure S4). This peak is also seen with *in-situ* monitoring of the reaction in deuterated sulfuric acid in Figure 1b (note the chemical shift is shifted upfield due to high concentration of acid). In addition, a second new peak appears at 9.85–10.1 ppm, shifting downfield and increasing in intensity as deconstruction progresses. This peak is assigned to residual HSO_4^- that is trapped in the newly formed pores of the deconstructed polymer[21] (refer to Figure S9 and Figure S10 for additional confirmation). As deconstruction advances, the polymer matrix swells slowly, enabling larger volumes of acid to penetrate through the polymer chains; this acid is then captured during the reaction quenching process. The increase in residual acid intensity is supplementary evidence that the system undergoes molecular swelling and expansion, with increased porosity. This swelling is further discussed below in the context of NMR relaxation and diffusion.

Polymer deconstruction in HBr acid leads to the evolution of a distinct proton environment at 8–9 ppm. Given the

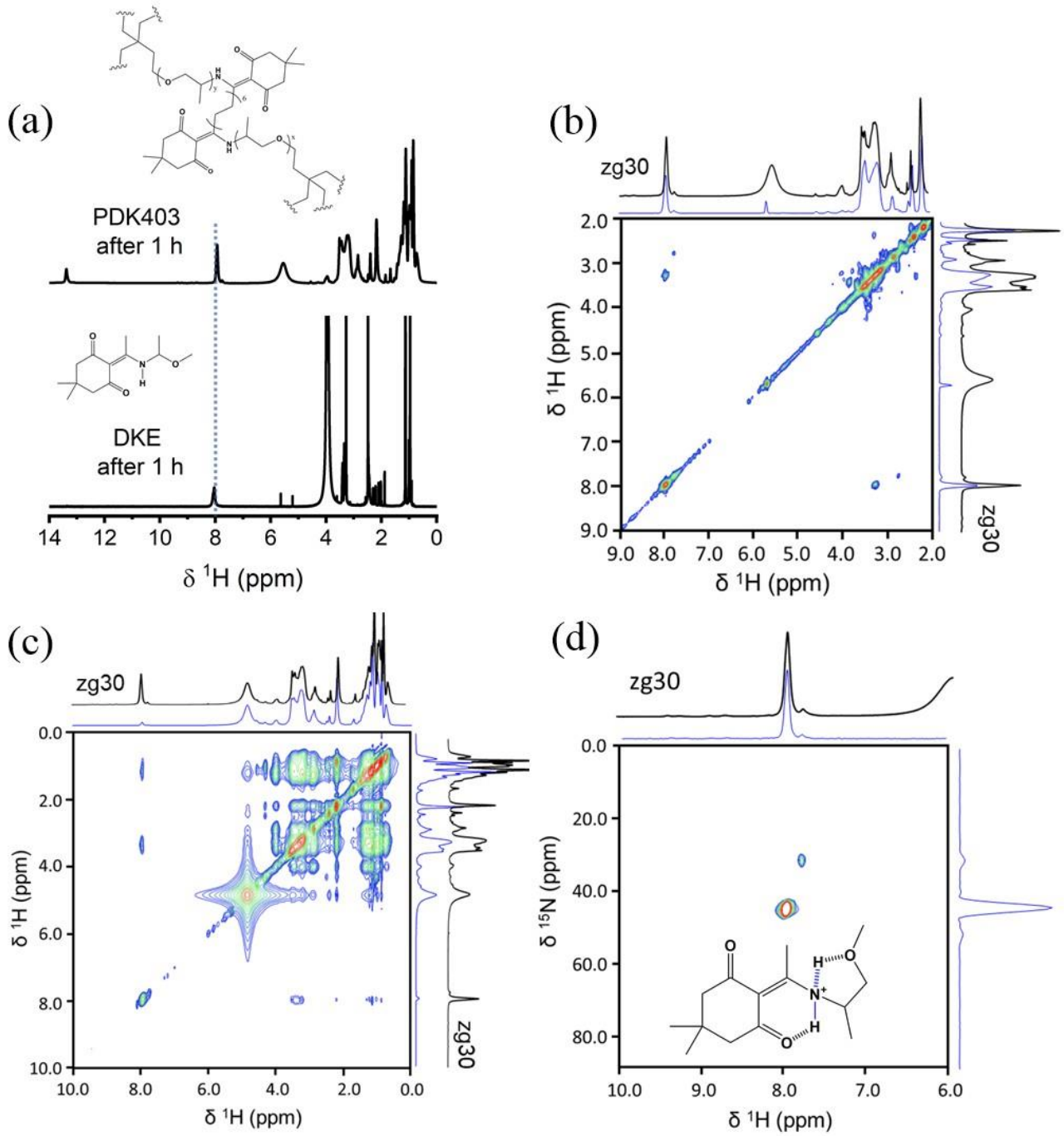

Figure 3. (a) ^{1}H spectra of recovered DKE after 1 h in 5 M HCl, extracted with DMSO-d_6 (bottom spectrum) and solid sample of recovered PDK403 after 1 h in 5 M HBr dissolved in DMSO-d_6. (b) ^{1}H–^{1}H COSY measurement of recovered polymer after 1 h in 5 M HBr dissolved in DMSO-d_6. A cross peak can be seen between ^{1}H at 8 ppm and ^{1}H at 3.4 ppm, assigned to CH_2-O site. (c) ^{1}H–^{1}H NOESY measurement of recovered polymer after 1 h in 5 M HBr dissolved in DMSO-d_6. Two cross peaks with 8 ppm are evidenced: the first correlates with 3.4 ppm, assigned to CH_2-O site The second cross peak correlates ^{1}H at 8 ppm with 1.2 ppm, assigned to hydrocarbon group of the methylene chain. (d) ^{1}H–^{15}N HSQC correlation of recovered polymer 1 h in 5 M HBr dissolved in DMSO-d_6. Inset shows the proposed structure of the intermediate material formed during deconstruction. Central cross peak is attributed to the ^{15}N-H-O site at 45 ppm correlating with ^{1}H at 8 ppm as discussed in the main text and SI. Spectra were acquired at 11.7 T.

efficient protonation abilities of the amine reaction site, we suggest that the 8–9 ppm peak is associated with the formation of a rather stable intermediate that remains in the reaction medium even after 5 h of deconstruction time. This intermediate is also formed in the deconstruction of additional PDK formulations with structurally similar

crosslinkers, but varying in molar mass (Figure S11) and does not change with varying temperature or after a base treatment (Figure S12 and S13), demonstrating its relative stability. The question remains as to the identity of an intermediate that presents itself as an ~8 ppm proton NMR peak in HBr depolymerization.

A comparative study of the deconstruction of PDK403 and the equivalent small molecule, diketonenamine (DKE) in acid was conducted. Figure 3a presents ^{1}H spectra of recovered small molecule and polymer after 1 h in acid solution, showing a clear presence of the 8 ppm proton environment. ^{1}H–^{1}H 2D COSY and NOESY measurements were performed for both samples, with comparable cross peaks (Figures 3b-3c, S15–S16). The proton environment is coupled through bonds to the proton adjacent to the ether group, CH_2-O-CH_2, and through space to the protons in the methylene chain (see SI for detailed cross peak data and Figure S17). ^{1}H–^{13}C HSQC experiments did not show any cross peaks, suggesting an OH or NH bond.

Figure 3d displays a ^{1}H–^{15}N HSQC spectrum acquired from deconstructed PDK403 after 1 h in HBr acid (full chemical shift range of the 2D correlation is found in Figure S18-19). Two cross peaks are observed: ^{1}H at 7.8 ppm correlated to ^{15}N at 32 ppm, and ^{1}H at 8 ppm correlated to ^{15}N at 45 ppm. DFT calculations for suspected chemical structures of reaction intermediates were performed and are summarized in Table S1. Based upon these calculations, the first smaller cross peak is assigned to a protonated primary amine;[22] this is further supported by ^{15}N chemical shift of T403 that resonates at 34 ppm (Figure S20). The second cross peak is assigned to the hydrogen–nitrogen bond in the proposed structure in the inset of Figure 3d (see SI and Table S2 for detailed analysis). Intramolecular hydrogen bonding of five-membered rings in benzoxazines, reported to resonate at 8.4 ppm, leads to enhanced stability of this structure.[23,24] The additional oxygen–hydrogen bond maintains the structure of the intermediate state, further stabilized by a solvation shell of the counter ion, resulting in enhanced stability evidenced by its presence even after 5 h of deconstruction in 5 M HBr acid. This intermediate is not a byproduct; it is present in the polymer matrix and can disappear as deconstruction progresses, enabling elimination of the protonated amine and further monomer formation. However, its stability may lead to inhibition of the deconstruction process. Monitoring the presence of this intermediate as a function of reaction time yields insight.

Quantitative ^{1}H high-speed MAS Hahn echo spectra (Figure 2c and 2d) were deconvoluted, separating the proton environments into four groups, according to their chemical shift and peak linewidth. Broad peaks, with chemical shifts originating from PDK403, were designated as "polymer"; peaks resonating at 7.3-7.6 ppm were grouped as "NH^+"; "Intermediate / HBr" was assigned to peaks at 8-8.5 ppm; narrow, sharp peaks were grouped as "monomer" (Figure S23). Figure 4a shows the proton populations of the designated groups for recovered PDK403 samples as a function of deconstruction time, in both 5 M HBr (blue) and 5 M H_2SO_4 (red) systems (for numeric percentages see Table S3). The protonated diketoenamine bond (NH^+) is evident

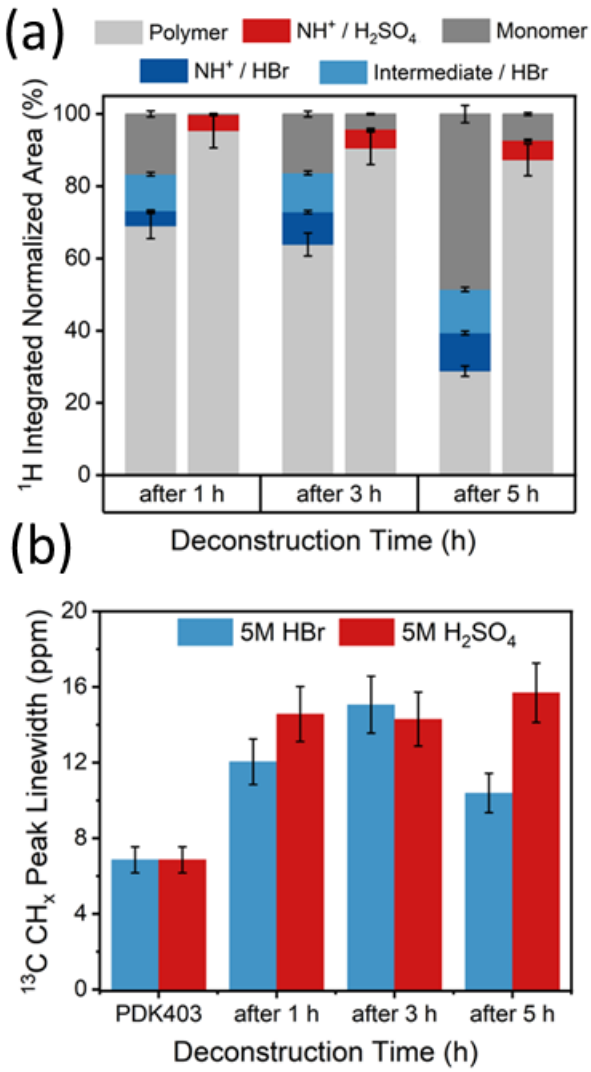

Figure 4. (a) Integration of deconvoluted normalized ^{1}H Hahn echo spectra (Figure 2c and 2d) of recovered PDK403 in 5 M HBr (blue) and 5 M H_2SO_4 (red) acid solutions as a function of deconstruction time. (b) Peak linewidth of ^{13}C chemical shift region of 0–30 ppm, corresponding to carbon resonance from polymer chains, was fit and plotted vs deconstruction time in 5 M HBr acid (blue) and H_2SO_4 acid (red).

after 1 h reaction in acid and slowly increases with deconstruction time. Monomer formation in HBr is apparent already after 1 h, stays stable after 3 h, and greatly increases after 5 h. It is noteworthy that the intermediate group (cyclic hydrogen bond structure) is constant throughout the deconstruction process (~10%), suggesting complex molecularity. Nonetheless, after 5 h in HBr, there is still 30% of NMR intensity associated with polymer-like proton environments that have not reacted. It is important to note that this polymer-like proton signal is not pristine PDK403 situated in the inner part of the cylindrical piece, where acid cannot or has not penetrated yet (see Method and Materials section for more details on sample preparation). In comparison to HBr, deconstruction in 5 M H_2SO_4 yields less monomer formation throughout the process, with a constant

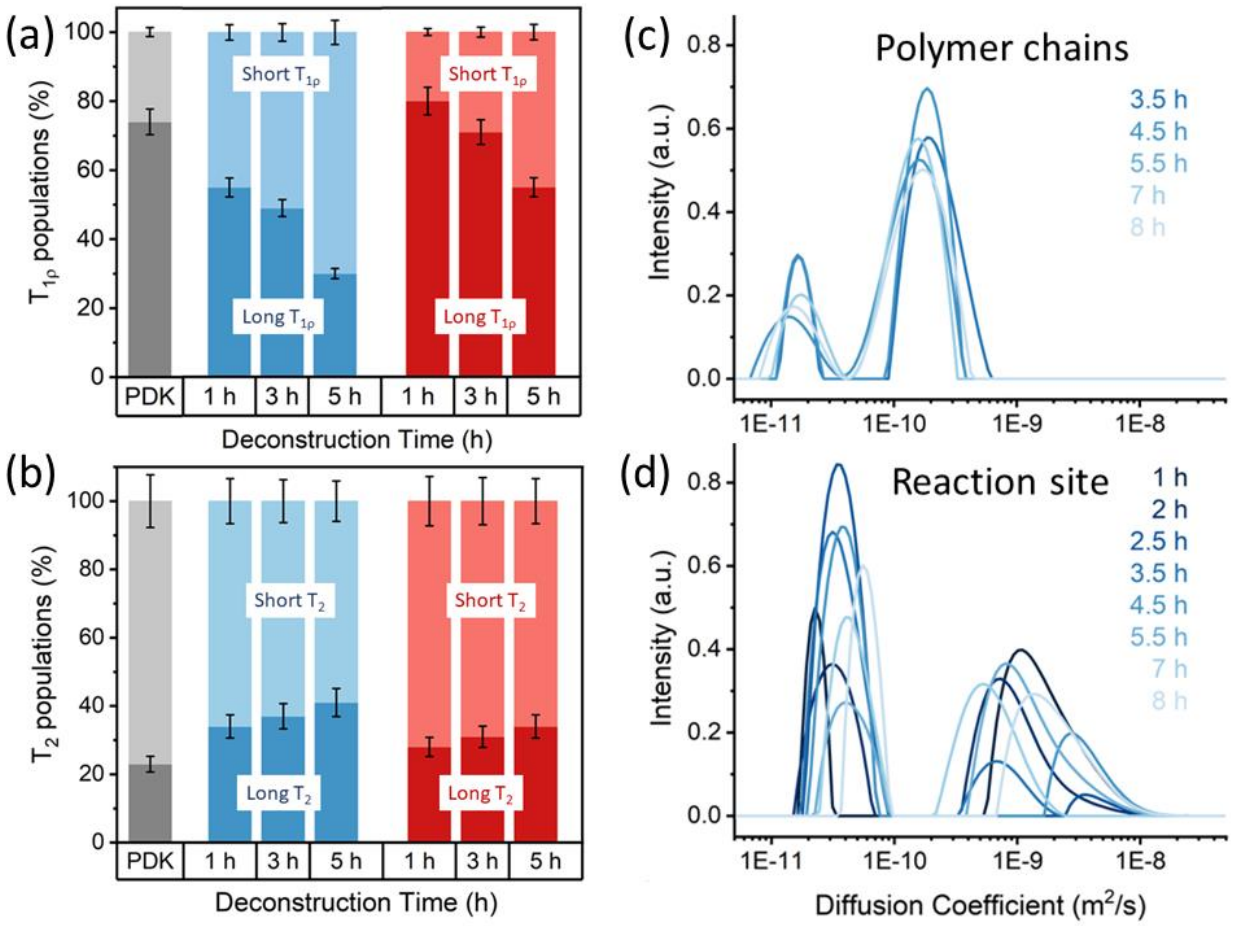

Figure 5. (a) ^{1}H $T_{1\rho}$ populations and (b) ^{1}H T_2 populations of PDK403 and deconstructed polymer in 5 M HBr (blue) and 5M H_2SO_4 (red). Long relaxation is represented with dark color shade and short relaxation with lighter color shade. ^{1}H $T_{1\rho}$ measurements were acquired with a spin lock field of 80 kHz. Distribution of diffusion coefficients (measured with ^{1}H PFG-NMR) analyzed with inverse Laplace transform as a function of PDK403 deconstruction time in 5 M DBr/D_2O (c) for reaction active site (-NH^+-) proton environment and (d) for polymer chains (-CH_2-) proton environment.

percentage of -NH^+ intermediate throughout the reaction (~8%). This is consistent with polymer deconstruction in H_2SO_4 being much slower than the deconstruction rate in HBr.

Figure 4b tracks the change in ^{13}C peak linewidth as a function of deconstruction time of the polymer chain environment (Figure 2a and 2b). We correlate the increase in linewidth to swelling of polymer chains on the microscopic level where relaxation and/or spectral dispersion broadens lines. Macroscopic chain swelling has been reported to occur upon polymer immersion in acid,[15,16] leading to a distribution of ^{13}C chemical environments and broadened peak linewidths. An alternative rationale, given that the samples were quenched and dried, is that line broadening is associated with amorphous chain packing. As the reaction proceeds past three hours, polymer chain linewidth decreases, particularly for the HBr-catalyzed system. This is presumed to be associated with increased mobility of the monomer-like CH_x bonds, further supporting the enhanced deconstruction rate of PDK in HBr acid medium. In comparison, broadening of the CH_x chain region is seen over the course of 5 h in H_2SO_4 and presumably continues. This supports the hypothesis of slow chain swelling in H_2SO_4 which can lead to larger pores and acid entrapment.

Considering the data presented above, we propose the following mechanistic insight (Figure S24): acidolysis of the polymer in 5 M HBr acid occurs in a swelled matrix, under stress and strain of the polymer chains. Protonation of the nitrogen leads to an activated diketoenamine bond which can further form a stable intermediate. The stretching and strain of swelling, distorts the hydrogen bonds of the stable intermediate, resulting in further formation of an iminium bond, water attack, and monomer generation. As chain deconstruction progresses, the matrix begins to break, resulting in an unreactive conformation for the intermediate which sterically hinders access to the protonated NH^+-C bond. The unreactive intermediate stays constant throughout the deconstruction process, most likely as a relatively stable untethered arm. In contrast, the kinetics of polymer acidolysis in 5 M H_2SO_4 are much slower, enabling longer swelling times and increased porosity.

In summary, these NMR methods applied to acid deconstruction of PDK explain the chemistry shown in Figure 1a, with the formation of a protonated reaction intermediate at

the amine site in PDK deconstruction in HBr that persists throughout the deconstruction process. The reactivity of the intermediate is greatly affected by the polymer chain dynamics during matrix expansion and swelling, and final chain deconstruction. We next turn to characterization of the motional dynamics of the residual polymers to further understand the implications of chain mobility on the reactivity of deconstruction.

Molecular Motion and Reactivity throughout Polymer Deconstruction

The linewidths shown in Figure 4b reflect the relaxation rates R_2^* (=$1/T_2^*$) and thus are influenced by molecular motion with longer relaxation times associated with increased mobility (longer T_2^* and narrow lines).[25] Measurements of spin-lattice relaxation in the rotating frame ($R_{1\rho} = 1/T_{1\rho}$) are also sensitive probes of molecular motion on the timescale of ms–s, corresponding to spin-lock frequencies of a few Hz to a few kHz.[26] Faster rotating frame relaxation rates (shorter $T_{1\rho}$) are associated with increased molecular motion. For longer T_2 and shorter $T_{1\rho}$ relaxation to be associated with increased mobility, one has to be on the right of the $\tau_c\omega_0$ minimum, with increased motion resulting in shorter correlation times.[27] Finally, pulsed field gradient diffusion measurements (PFG-NMR) probe longer length scale motion of chemical moieties in an applied magnetic field gradient. Here the derived "self-diffusion coefficient" D (dimensions of m^2/s) quantitates the macroscopic motion where larger D corresponds to faster motion. We examine all these measurements for the HBr and H_2SO_4 deconstruction reactions.

Figure 5a shows our analysis of ^{1}H spin lattice relaxation times in the rotating frame ($T_{1\rho}$) of the polymer samples during the first 5 h of deconstruction (see Table S4 for nominal results); nominal analysis of these rates produces bi-exponential decays shown as the ratio between the populations of slow and fast ^{1}H $T_{1\rho}$ relaxation times. From the point of view of polymer motion, pristine PDK403 consists of two dynamic regimes, 26% with more rapid relaxation (530 μs) corresponding to faster motion and 74% with slower relaxation (2.5 ms) corresponding to slower motion. As deconstruction proceeds in HBr acid, harvested residual polymer shows an increasing fraction of the region associated with short $T_{1\rho}$ values, i.e., faster relaxation rates and more rapid motion. We submit here, monomer formation occurs, leading to the presence of fast-moving smaller chains. Further supporting evidence of the fast motion regime can be seen in Figure 5b, portraying the increase in ^{1}H T_2 values as deconstruction proceeds (nominal T_2 relaxation results can be found in Table S5).

The ratio of populations associated with slow and fast motion as a function of deconstruction time agrees with the fractional line shape analysis portrayal shown in Figure 4a (Figure S25). A similar trend is observed for the relative segments of fast and slow ^{1}H $T_{1\rho}$ relaxation times of deconstructed samples in 5 M H_2SO_4, though the increase in population of faster moving polymer chains is more gradual in time due to slower deconstruction kinetics in this system. However, two distinct domains of motion, with the higher mobility fraction increasing with deconstruction time, are clearly observed for all deconstructed samples, further supporting the dynamic morphological heterogeneity of the deconstruction process. It should be noted that ^{1}H $T_{1\rho}$ relaxation times presented here, equivalent to local motion in the samples, are averaged over the entire sample volume, without chemical specificity. Figure S26 shows a normalized comparison of linewidths and relaxation rates for the HBr and H_2SO_4 residual polymers where the trend for increased regions of polymer mobility in the residual products is clear.

Self-diffusion measurements in-situ of the acid deconstruction process are shown in Figure 5c and 5d. Measurements were performed over a course of ~ 8 h of deconstruction, utilizing multi-exponential Inverse Laplace transform (ILT)[28] to analyze the attenuation of the ^{1}H PFG-NMR signal, resulting in a distribution of the translational self-diffusion coefficients (D) for the specific proton chemical environments. Figure 5c and 5d show the distributions of D for the protons in CH_2 polymer chains (integration of peak at 0.8 – 1.5 ppm) and for the reaction site (protonated amine group, integration of peak at 7.5 – 8.5 ppm), as a function of reaction time in DBr/D_2O, respectively. Both functional groups exhibit bimodal distributions of self-diffusion coefficients D.

Polymer chain diffusion (Figure 5c) can be parsed into two domains of motion, with average diffusion coefficients of $1.7*10^{-10}$ m^2 s^{-1} and $1.6*10^{-11}$ m^2 s^{-1}. We assign the slower motion to semi-ordered, unreacted polymer chains that remain largely unaffected during the reaction time. The larger self-diffusion coefficient can be assigned to polymer chains that are "splaying" as the reaction proceeds, hence presenting increased local mobility. Further assessment of the mobility of a swelled polymer matrix was performed by monitoring PDK403 in different solvents and can be found in Table S6. Concentrated acid shows better polymer swelling capabilities than pure D_2O, and consequently faster self-diffusion, but inferior to swelling properties of an organic solvent like chloroform.

The reaction site (Figure 5d) also presents two regions of local motion where the slower component likely arises from the strong effect of the polymer backbone. Indeed, the distribution of this slower D is the average of the slow and moderate polymer chain motions, seen in Figure 5c. The faster self-diffusion coefficient is on the same order of magnitude as H_3O^+ molecular diffusion[15] measured during deconstruction of DKE. This enhanced mobility results from increased movement of protons at the reaction site that undergo fragmentation and exhibit escalated free motion in the acid solution. (Further discussion of the ILT analysis and ratio of the fast and slow motions as a function of deconstruction time can be found in the supporting information and Figures S27-30).

It should be noted that the deconstruction time dependence of the diffusion coefficients is not straightforward and does not show a clear increase or decrease of D in time. The non-linearity of the molecular diffusivity and the complexity of the deconstruction process result from the intercalation of different factors affecting the deconstruction, such as swelling, diffusion and reaction. Correlation of polymer

deconstruction with fractal kinetics has been reported recently,[16] where fractal-based equations are employed to parameterize rate laws. Nonetheless, the diverse, heterogeneous essence of polymer motion throughout the deconstruction process is clear. In our analyses, the slow diffusive motion of the rigid polymer chains greatly affects the motion of the reaction site, at times being the dominant motion measured, while the fast mobility of the reaction site steers the hydrolysis forward. These results provide experimental evidence supporting a multi-pathway deconstruction mechanism in HBr, shedding light on the importance of local chain dynamics and its control over the reactivity and stability of the formed intermediate.

CONCLUSIONS

Heterogenous deconstruction of a model elastomer featuring acid-cleavable diketoenamine bonds is presented in 5 M HBr and H_2SO_4 acid solutions, with the advancement and application of magnetic resonance methodologies offering insights.

Polymer deconstruction is complex and not uniform: different regions of the polymer begin to react, becoming more susceptible to acid penetration, while other regions remain unaffected by the contact with acid. Although monomer formation is evident even at early stages of the deconstruction process, remnants of polymer can be seen even after 5 h in both HBr and H_2SO_4 concentrated acid systems.

On the molecular level, it is clear that deconstruction in HBr is faster than in H_2SO_4 acid solution. We show clear evidence of different deconstruction mechanisms in these acids. The chaotropic nature of HBr facilitate the high mobility of the reaction site, prompting formation of a rather stable intermediate and necessitating an additional energy barrier for completion of the reaction. Stretching and strain during polymer matrix swelling promotes the reactive conformation of the intermediate, resulting in monomer formation. After chain deconstruction occurs, the intermediate remains in its stationary form. The diffusivity behavior of the reaction site, strongly linked to the moderate-to-slow kinetics of the polymer chains further demonstrates this complex polymer deconstruction process. To promote a reactive configuration for deconstruction, chain dynamics need to be addressed. In contrast, slow deconstruction kinetics of the polymer follows from slower swelling in H_2SO_4, enabling emerging porosity of the polymer and acid entrapment within.

The ability to understand reaction mechanisms allows refinement of deconstruction conditions. We submit that enhanced local chain mobility is critical to ensure reactive configurations and fast and clean polymer deconstruction; such local mobilities can be controlled with material design e.g., by the addition of heteroatoms in the polymer backbone.

We conclude that NMR methodologies provide molecular insight into polymer deconstruction by relating local structure to molecular mobility, thereby adding further guidance in the planning and production of future circular materials.

ASSOCIATED CONTENT

Supporting Information. The supporting information is available free of charge via the Internet at http://pubs.acs.org.
Detailed material and sample preparation; characterization methods; supplementary NMR measurements; small molecule 2D NMR measurements; molecular structure and DFT calculations for proposed ^{1}H-^{15}N crosspeaks; nominal data for ^{1}H T_2 and $T_{1\rho}$ measurements and ^{1}H integrated intensities, and ^{1}H PFG-NMR in-depth discussion. NMR raw data is available at https://doi.org/10.5061/dryad.n8pk0p34g.

AUTHOR INFORMATION

Corresponding Author

* Shira Haber email: shirahaber.lbl@gmail.com
* Jeffrey A. Reimer email: reimer@berkeley.edu

Present Addresses

†Yusuf Hamied Department of Chemistry, University of Cambridge, Lensfield Road, Cambridge, UK CB2 1EW.

Author Contributions

The CRediT author contributions are as follows:
S.H., J.A.R., S.N.F., M.H., and B.A.H. contributed to the conceptualization of the project. S.H. and J.A.R. contributed to the design of the project. M.H. contributed to the design of PDK elastomers and DKE materials. A.R.E. performed all DFT simulations. NMR characterization and analysis was performed by S.H. and J.I. ILT analysis for PFG-NMR was performed by J.I. Further NMR methodology and development was performed by S.H., R.G., and H.C. S.H., J.I., A.R.E., S.N.F., and M.H. contributed to visualization. S.H. wrote the original draft. J.I. wrote the PFG-NMR discussion with S.H. supervision. All authors contributed to the final draft and editing. J.A.R., B.A.H., and K.A.P. supervised research, provided project administration, and acquired funding.

Notes

Competing interests: The authors declare the following competing interests: B.A.H. is an inventor on the US provisional patent application 62/587,148 submitted by Lawrence Berkeley National Laboratory that covers PDKs, as well as aspects of their use and recovery. B.A.H. and M.H. are inventors on the US provisional patent application 63/390,962 submitted by Lawrence Berkeley National Laboratory that covers biorenewable PDKs, as well as aspects of their use and recovery. B.A.H. has a financial interest in Cyklos Materials and Sepion Technologies. The remaining authors declare no competing interests.

ACKNOWLEDGMENT

This work was funded by the U.S. Department of Energy, Office of Science, Office of Basic Energy Sciences, Materials Sciences and Engineering Division under contract no. DE-AC02-05-CH11231, Unlocking Chemical Circularity in Recycling by Controlling Polymer Reactivity across Scales program CUP-LBL-Helms. Work at the Molecular Foundry, polymer and small molecule synthesis and characterization, was done and supported by the Office of Science, Office of Basic Energy Sciences, of the U.S. Department of Energy under Contract No. DE-AC02-05CH11231. S.N.F. gratefully acknowledges support as a Pines Magnetic Resonance Center Postdoctoral Fellow.
We thank Pines Magnetic Resonance Center's Core NMR Facility (PMRC Core) for spectroscopic resources used in this study.

The instrument used in this work for ^{1}H PFG-NMR measurements and variable temperature ^{1}H NMR measurements is supported by the National Science Foundation under Grant No. 2018784. The instrument used for acquiring ^{15}N measurement of T403 monomer and selective ^{1}H NOESY measurements is supported in part by NIH S10OD024998. This research used the Savio computational cluster resource provided by the Berkeley Research Computing program at the University of California, Berkeley (supported by the UC Berkeley Chancellor, Vice Chancellor for Research, and Chief Information Officer). We thank Norman Su and Huntsman Corp. for providing the triamine monomers used in the study.

REFERENCES

(1) Helms, B. A. Polydiketoenamines for a Circular Plastics Economy. *Acc Chem Res* **2022**, *55* (19), 2753–2765. https://doi.org/10.1021/acs.accounts.2c00308.

(2) Häußler, M.; Eck, M.; Rothauer, D.; Mecking, S. Closed-Loop Recycling of Polyethylene-like Materials. *Nature* **2021**, *590* (7846), 423–427. https://doi.org/10.1038/s41586-020-03149-9.

(3) Abel, B. A.; Snyder, R. L.; Coates, G. W. Chemically Recyclable Thermoplastics from Reversible-Deactivation Polymerization of Cyclic Acetals. *Science (1979)* **2021**, *373*, 783–789.

(4) Coates, G. W.; Getzler, Y. D. Y. L. Chemical Recycling to Monomer for an Ideal, Circular Polymer Economy. *Nature Reviews Materials*. Nature Research July 1, 2020, pp 501–516. https://doi.org/10.1038/s41578-020-0190-4.

(5) Beedle, A. E. M.; Mora, M.; Davis, C. T.; Snijders, A. P.; Stirnemann, G.; Garcia-Manyes, S. Forcing the Reversibility of a Mechanochemical Reaction. *Nat Commun* **2018**, *9* (1), 3155.

(6) Christensen, P. R.; Scheuermann, A. M.; Loeffler, K. E.; Helms, B. A. Closed-Loop Recycling of Plastics Enabled by Dynamic Covalent Diketoenamine Bonds. *Nat Chem* **2019**, *11* (5), 442–448. https://doi.org/10.1038/s41557-019-0249-2.

(7) Demarteau, J.; Cousineau, B.; Wang, Z.; Bose, B.; Cheong, S.; Lan, G.; Baral, N. R.; Teat, S. J.; Scown, C. D.; Keasling, J. D.; Helms, B. A. Biorenewable and Circular Polydiketoenamine Plastics. *Nat Sustain* **2023**, *6* (11), 1426–1435. https://doi.org/10.1038/s41893-023-01160-2.

(8) Chu, M.; Liu, Y.; Lou, X.; Zhang, Q.; Chen, J. Rational Design of Chemical Catalysis for Plastic Recycling. *ACS Catalysis*. American Chemical Society April 15, 2022, pp 4659–4679. https://doi.org/10.1021/acscatal.2c01286.

(9) Young, J. B.; Hughes, R. W.; Tamura, A. M.; Bailey, L. S.; Stewart, K. A.; Sumerlin, B. S. Bulk Depolymerization of Poly(Methyl Methacrylate) via Chain-End Initiation for Catalyst-Free Reversion to Monomer. *Chem* **2023**, *9* (9), 2669–2682. https://doi.org/10.1016/j.chempr.2023.07.004.

(10) Ellis, L. D.; Rorrer, N. A.; Sullivan, K. P.; Otto, M.; McGeehan, J. E.; Román-Leshkov, Y.; Wierckx, N.; Beckham, G. T. Chemical and Biological Catalysis for Plastics Recycling and Upcycling. *Nature Catalysis*. Nature Research July 1, 2021, pp 539–556. https://doi.org/10.1038/s41929-021-00648-4.

(11) Metze, F. K.; Sant, S.; Meng, Z.; Klok, H. A.; Kaur, K. Swelling-Activated, Soft Mechanochemistry in Polymer Materials. *Langmuir*. American Chemical Society March 14, 2023, pp 3546–3557. https://doi.org/10.1021/acs.langmuir.2c02801.

(12) Lee, C. K.; Diesendruck, C. E.; Lu, E.; Pickett, A. N.; May, P. A.; Moore, J. S.; Braun, P. V. Solvent Swelling Activation of a Mechanophore in a Polymer Network. *Macromolecules* **2014**, *47* (8), 2690–2694. https://doi.org/10.1021/ma500195h.

(13) Demarteau, J.; Epstein, A. R.; Christensen, P. R.; Abubekerov, M.; Wang, H.; Teat, S. J.; Seguin, T. J.; Chan, C. W.; Scown, C. D.; Russell, T. P.; Keasling, J. D.; Persson, K. A.; Helms, B. A. Circularity in Mixed-Plastic Chemical Recycling Enabled by Variable Rates of Polydiketoenamine Hydrolysis. *Sci. Adv* **2022**, *8*, 8823.

(14) Epstein, A. R.; Demarteau, J.; Helms, B. A.; Persson, K. A. Variable Amine Spacing Determines Depolymerization Rate in Polydiketoenamines. *J Am Chem Soc* **2023**, *145* (14), 8082–8089. https://doi.org/10.1021/jacs.3c00772.

(15) Hua, M.; Peng, Z.; Guha, R.; Ruan, X.; Ng, K. C.; Demarteau, J.; Haber, S.; Fricke, S. N.; Reimer, J. A.; Salmeron, M.; Persson, K. A.; Wang, C.; Helms, B. A. Mechanochemically Accelerated Deconstruction of Chemically Recyclable Plastics. *ChemRxiv* **2023**. https://doi.org/10.26434/chemrxiv-2023-rf93d.

(16) Fricke, S. N.; Haber, S.; Hua, M.; Salgado, M.; Helms, B. A.; Reimer, J. A. Magnetic Resonance Insights into the Heterogeneous, Fractal-like Kinetics of Chemically Recyclable Polymers. *Sci. Adv* **2024**, *10*, 568.

(17) Bruce, E. E.; Van Der Vegt, N. F. A. Molecular Scale Solvation in Complex Solutions. *J Am Chem Soc* **2019**, *141* (33), 12948–12956. https://doi.org/10.1021/jacs.9b03469.

(18) Johnson, R. L.; Schmidt-Rohr, K. Quantitative Solid-State 13C NMR with Signal Enhancement by Multiple Cross Polarization. *Journal of Magnetic Resonance* **2014**, *239*, 44–49. https://doi.org/10.1016/j.jmr.2013.11.009.

(19) Liu, H.; Zhou, X.; Chen, Q.; Zhang, S. Accurate Quantitative and Maximum Cross Polarization via Multiple Ramped Contacts. *Chem Phys Lett* **2017**, *679*, 233–236. https://doi.org/10.1016/j.cplett.2017.05.009.

(20) Brownbill, N. J.; Sprick, R. S.; Bonillo, B.; Pawsey, S.; Aussenac, F.; Fielding, A. J.; Cooper, A. I.; Blanc, F. Structural Elucidation of Amorphous Photocatalytic Polymers from Dynamic Nuclear Polarization Enhanced Solid State NMR. *Macromolecules* **2018**, *51* (8), 3088–3096. https://doi.org/10.1021/acs.macromol.7b02544.

(21) Batamack, P.; Fraissard, J. Proton NMR Studies on Concentrated Aqueous Sulfuric Acid Solutions and Nafion-H. *Catal Letters* **1997**, *49*, 129–136.

(22) Lambert, J. B.; Binsch, G.; Roberts, J. D. Nitrogen-15 Magnetic Resonance Spectroscopy. I. Chemical Shifts. *Proc Natl Acad Sci U S A* **1964**, *51*, 735–737. https://doi.org/10.1073/pnas.51.5.735.

(23) Hansen, P. E. A Spectroscopic Overview of Intramolecular Hydrogen Bonds of NH … O,S,N Type. *Molecules* **2021**, *26* (9), 2409. https://doi.org/10.3390/molecules26092409.

(24) Froimowicz, P.; Zhang, K.; Ishida, H. Intramolecular Hydrogen Bonding in Benzoxazines: When Structural Design Becomes Functional. *Chemistry - A European Journal* **2016**, *22* (8), 2691–2707. https://doi.org/10.1002/chem.201503477.

(25) Horii, F. Chapter 3 NMR Relaxations and Dynamics. In *Solid State NMR of Polymers*; Ando, I., Asakura, T., Eds.; Elsevier Science B.V, 1998; Vol. 84.

(26) Kowalewski, J.; Mäler, L. *Nuclear Spin Relaxation in Liquids : Theory, Experiments, and Applications*, 6th ed.; Taylor & Francis,: New York, 2006.

(27) Fukushima, Eiichi.; Roeder, S. B. W. *Experimental Pulse NMR : A Nuts and Bolts Approach*; Addison-Wesley Pub. Co., Advanced Book Program, 1981.

(28) Hansen, P. C.; Jensen, T. K.; Rodriguez, G. An Adaptive Pruning Algorithm for the Discrete L-Curve Criterion. *J Comput Appl Math* **2007**, *198* (2), 483–492. https://doi.org/10.1016/j.cam.2005.09.026.